Published in final edited form as:

J Control Release. 2016 August 28; 236: 31–37. doi:10.1016/j.jconrel.2016.06.020.

Nanoparticle-mediated miR200-b delivery for the treatment of diabetic retinopathy

Rajendra Narayan Mitra[a], **Chance A. Nichols**[b], **Junjing Guo**[b], **Rasha Makkia**[b], **Mark J. Cooper**[d], **Muna I. Naash**[b,c], and **Zongchao Han**[a,e,f,*]

[a]Department of Ophthalmology, University of North Carolina, Chapel Hill, NC 27599, USA

[b]Department of Cell Biology, University of Oklahoma Health Sciences Center, Oklahoma City, OK 73104, USA

[c]Department of Biomedical Engineering, University of Houston, Houston, TX 77204, USA

[d]Copernicus Therapeutics, Incorporated, Cleveland, OH 44106, USA

[e]Carolina Institute for NanoMedicine, University of North Carolina, Chapel Hill, NC 27599, USA

[f]Division of Molecular Pharmaceutics, Eshelman School of Pharmacy, University of North Carolina, Chapel Hill, NC 27599, USA

Abstract

We recently reported that the *Ins2*^{Akita} mouse is a good model for late-onset diabetic retinopathy. Here, we investigated the effect of miR200-b, a potential anti-angiogenic factor, on VEGF receptor 2 (VEGFR-2) expression and to determine the underlying angiogenic response in mouse endothelial cells, and in retinas from aged *Ins2*^{Akita} mice. MiR200-b and its native flanking sequences were amplified and cloned into a pCAG-eGFP vector directed by the ubiquitous CAG promoter (namely pCAG-miR200-b-IRES-eGFP). The plasmid was compacted by CK30PEG10K into DNA nanoparticles (NPs) for *in vivo* delivery. Murine endothelial cell line, SVEC4-10, was first transfected with the plasmid. The mRNA levels of VEGF and VEGFR-2 were quantified by qRT-PCR and showed significant reduction in message expression compared with lipofectamine-transfected cells. Transfection of miR200-b suppressed the migration of SVEC4-10 cells. There was a significant inverse correlation between the level of expression of miR200-b and VEGFR-2. Intravitreal injection of miR200-b DNA NPs significantly reduced protein levels of VEGFR-2 as revealed by western blot and markedly suppressed angiogenesis as evaluated by fundus imaging in aged *Ins2*^{Akita} mice even after 3 months of post-injection. These findings suggest that NP-mediated miR200-b delivery has negatively regulated VEGFR-2 expression *in vivo*.

Keywords

Diabetic retinopathy; Angiogenesis; miR200-b; Nanoparticles; VEGF receptors

*Corresponding author at: University of North Carolina at Chapel Hill, Department of Ophthalmology, 2208 Marsico Hall, 125 Mason Farm Rd, Chapel Hill, NC 27599, USA. zongchao@med.unc.edu (Z. Han).

The remaining authors declare no conflicts of interest.

1. Introduction

Diabetic retinopathy (DR) is a highly specific retinal microvascular complication of diabetic patients worldwide and continues to be the leading cause of blindness among working age Americans [1–3]. In diabetes, hyperglycemia is a key stimulating factor for severe metabolic changes in vascular endothelial (EC) cells and results in vascular injuries [3,4]. The compromised stability of EC cells recruits and activates different transcription factors and alters the expression of different growth factors, including vascular endothelial growth factor (VEGF), which in turn deteriorates the structure and function of the retina [5]. Recent studies have explored elevated VEGF levels in the intraocular space of patients with DR, which has been hypothesized as the primary pathogenic factor in the angiogenesis seen in DR [5–9]. VEGF is a heparin binding homodimeric glycoprotein that specifically binds to tyrosine kinase receptors (TKRs), VEGFR-1 (Flt 1, fms-like tyrosine kinase 1), VEGFR-2 (Flk-1, fetal liver kinase), or 1/KDR (kinase insert domain receptor) on the vascular EC surface [10]. These receptors direct different physiological (e.g. embryonic development) and pathological angiogenesis (e.g. DR, tumor progression, inflammation etc.). VEGFR-1 is expressed both in normal and diabetic retina and is responsible for organization of normal vascular channels. Studies show that the *Flt-1*$^{-/-}$ mice die in utero between 8.5 and 9.5 embryonic days due to disorganization of blood vessels [11,12]. VEGFR-2 is responsible for migration, proliferation and survival as well as stimulation of angiogenesis and vascular permeability at the late stage of DR (i.e. proliferative DR) [10]. Therefore, modulation of increased VEGF receptors and inhibition of their function in the eye may become a logical method of controlling normal vascular homeostasis, as well as a possible treatment for DR.

MicroRNAs (miRNAs) are a class of naturally occurring small and non-coding RNA molecules [13,14]. miRNA has been recognized as a key component in regulating cell differentiation, apoptosis, cell proliferation and organ development. More than 60% of human proteins are regulated by miRNAs [14]. It silences gene expression at the post-transcriptional level by base pairing with perfect or nearly perfect complementary 3′-untranslated region (3′-UTR) of the target mRNA that results in a cleavage of mRNA and translational repression occurs [14]. Therefore, it is hypothesized that dysregulation in the biogenesis and function of miRNAs may be involved in the pathogenesis of various human diseases, including DR. The miR200 family is established as an anti-angiogenic factor that can inhibit the growth of new blood vessels by down regulating VEGF [15,16]. Among all of the miR200 members, miR200-b is one of the most potent endogenous inhibitors involved in anti-angiogenesis and also is a well-studied therapeutic target as a tumor suppressor [16]. Although miR200-b has been successful in inhibiting VEGF gene expression *in vitro* and in *in vivo* models [15], its therapeutic delivery into the retina has not been extensively evaluated. Recently, the delivery of miR200-b was carried out using lipofectamine and with a dose of 1.4 μg/week (duration of 4 weeks) in streptozotocin (STZ)-induced diabetic rats which demonstrated that miR200-b has a negative role in regulating VEGF induced DR [15].

Gene therapy is a promising strategy for treating a number of disorders. This could be especially beneficial for patients for whom standard options won’t work or are not available. Although viral vector based gene delivery has been proven to be robust in gene delivery, it has several inherent concerns [17,18]. We have previously shown the effectiveness of

CK30PEG10K compacted DNA NPs in efficiently transfect retinal tissues [18–21]. The expression of the therapeutic gene can result in long-term expression, rescue retina cells, and improve phenotypes in different neurodegenerative models (ABCA4$^{-/-}$, RPE65$^{-/-}$, Rds$^{+/-}$, Rho$^{-/-}$ mice) [20,22–26]. Earlier research on these DNA NPs determined that an acetate counterion to lysine amines could compact plasmid DNA into a rod shape with an 8–11 nm diameter and a length proportional to the plasmid size [27,28]. These NPs have a tolerable safety profile with a lack of immunogenicity in the retina after delivery through intravitreal and subretinal routes, including multiple dosing [21,25,29]. Our strategy here is to intravitreally deliver CK30PEG10k compacted therapeutic miR200-b plasmid DNA to 6 month old diabetic *Ins2*^{Akita} mice and evaluate its therapeutic role against VEGF-mediated angiogenesis at 3 months post injection (PI-3 m). We show that a single NP-mediated miR200-b dose negatively regulates VEGFR-2 expression in the type 1 diabetic *Ins2*^{Akita} mouse model of DR and demonstrate phenotypic improvements at 3 months post intravitreal injection. This approach may lead to an effective anti-angiogenic therapy for DR.

2. Materials and methods

2.1. Animal husbandry

Ins2^{Akita} heterozygous male and female breeder pairs with C57BL/6 background were kindly provided by Dr. Jason Kim at the University of Massachusetts Medical School. All the breeding colonies under investigation were in the C57BL/6 background and maintained in cyclic light (12 L:12 D) condition with water and food. After the onset of diabetes, freshly prepared cages were provided to all of the mice due to diabetes associated polyuria. All of the experiments, under our investigation were approved by University of Oklahoma Health Science Center Institutional Animal Care and Use Committee (IACUC), and followed to the National Institute of Health Guide for the Care and Use of Laboratory Animals and the Association for Research in Vision and Ophthalmology resolution on the Use of Animals in Research (Rockville, MD, USA). Homozygote *Ins2*^{Akita} mice are postnatal lethal (rarely survive beyond 12 weeks of age). The diabetic phenotype is more severe and progressive in heterozygous males than in heterozygous females. Thus, only Akita heterozygous male mice were used in this study. Aged matched WT littermates were used as controls.

2.2. NP formulation and characterization

DNA NPs were synthesized as mentioned earlier [27,30]. Briefly, a 30-mer L-lysine polypeptide with N-terminal cysteine residue (CK30) was conjugated with 10 kDa polyethylene glycol maleimide (PEG-maleimide, 10 kDa) *via* thiol-maleimide bioconjugation. After counterion exchange with acetate, CK30-PEG10k-acetate was generated and used to condense the pCAG-miR200-b-IRES-eGFP plasmid DNA (Fig. S1) as unimolecularly compacted DNA NPs at N/P ratio of 2 using charge neutralization between peptide (positive charges from ammonium groups) and DNA (negative charges from phosphates). The NPs were taken in saline (endotoxin free) and concentrated to 4.3 μg DNA/μl.

2.3. Cell culture

The mouse EC line SVEC4-10 was purchased from ATCC, USA. The cells were cultured in Dulbecco's modified Eagle's medium (DMEM) supplemented with 10% fetal bovine serum (FBS) and 1× of antibiotics and antimycotics mixture (AA, 100× stock) to each liter of medium at pH 7.4. The cells were incubated at 37 °C and 5% CO_2 throughout the study.

2.4. Wound healing assay

The cells were grown at 50–60% confluence for 12–18 h before transfection. The EC cells were transfected with pCAG-miR200-b-IRES-eGFP plasmid DNA (2 μg) using transfecting agent (lipofectamin 2000, Invitrogen). Untreated cells were taken as negative control. The cells were incubated at 37 °C until attaining a monolayer with 100% confluence. p200 pipet tips were used to create a scratch through the cell monolayer. Fresh media was added to the plate and incubated again at 37 °C. After 24 h, phase-contrast images were acquired to track cell migration and wound closure phenotype.

2.5. Tube formation assay

SVEC4-10 cells were transfected with lipofectamine 2000 and pCAG-miR200-b plasmid DNA complexes in 6 well plates. After 24 h of transfection, 1×10^4 cells were transferred in 100 μl of growth factor reduced matrigel (356230, BD Bioscience) to pre-coated 12 well plates along with untreated negative control cells. Tube formation was visualized and demonstrated after 0 and 24 h of this seeding.

2.6. Intravitreal injections

Intravitreal injections were performed as previously described [31] in postnatal (P) 6 month old *Ins2*^{Akita} and age matched WT controls. Animals were first anesthetized by intramuscular injection of 85 mg/kg ketamine and 14 mg/kg xylazine (Butler Schein Animal Health, Dublin, OH). The cornea was then carefully penetrated using a 30-gauge needle to make a hole. A 35-gauge needle attached to a 10 μl Nanofil syringe (World Precision Instruments, Sarasota, FL, USA) was then inserted through the puncture site with visualization aided by use of an operating microscope (Carl Zeiss Surgical, Incorporated, Thornwood, NY, USA) to deliver pCAG-miR200-b NPs (2.0 μl, 4.3 μg/μl) or pCAG-IRES-GFP (mock, 2 μl 4.3 μg/μl in saline) into the vitreal cavity. A drop of triple antibiotic (Equate, Wal-Mart, Bentonville, AR, USA) ointment was applied on the corneal surface after this injection. Mice were placed on a 37 °C bed until fully awake. All of the *in vivo* analyses were carried out at PI-3 m and 3–5 mice per group were taken for injections.

2.7. Fundus photography (fluorescein angiography)

Fundus photographs were acquired following our earlier method with Micron III (Phoenix Research laboratories, Pleasanton, CA) imaging system [32,33]. Animals were first anesthetized by intramuscular injection of 85 mg/kg ketamine and 14 mg/kg xylazine (Butler Schein Animal Health, Dublin, OH). 100 μl of 1% fluorescein sodium (Sigma-Aldrich, St. Louis, MO) solution was then injected intraperitoneally. 1% Cyclogyl (cyclopentolate hydrochloride solution) was used to dilate the eyes and a drop of 2.5% methylcellulose (both from Pharmaceutical Systems, Inc., Tulsa, OK) was used on the

corneal surface. Photographs were acquired using white light or a filter with excitation at ~482 nm and emission at ~536 nm using commercially available software (StreamPix Software; Phoenix Research Laboratories).

2.8. Western blotting

Western blotting was performed using standard protocols [19,20]. Retina samples were separated from corneas and lenses followed by homogenization and lysis in extraction buffer (PBS pH 7.0 containing 1% triton-× 100, 5 mM EDTA, 5 mg/ml n-ethylmaleimide, and a standard protease inhibitor cocktail) by short sonication on ice. After the extraction, samples were centrifuged at 4 °C to precipitate insoluble materials and supernatants were collected in fresh tubes on ice. Concentrations of isolated proteins were measured by the Bio-Rad protein assay kit (calorimetric protein assay, Bradford assay, Bio-Rad, Hercules, CA). The anti-VEGF (ab46154) and Flk-1 (C-1158: sc-504) antibodies were purchased from Abcam and Santa Cruz, respectively. The protein samples were always kept on ice for subsequent analysis and were stored at −80 °C. Equal amounts of total protein were run and separated by 10% SDS-PAGE followed by transfer to PVDF membrane (Millipore, Inc., Billerica, MA). Membranes were blocked with 5% non-fat milk in TBST and then incubated with primary antibody (1:1000) overnight at 4 °C. Membranes were washed with 1×TBST (3 times; 10 min each) and then treated with HRP conjugated goat anti-rabbit IgG antibody (sc-2030, Santa Cruz) at 1:25,000 and incubated for 2 h at room temperature, and washed as earlier followed by visualization using SuperSignal West Dura Extended Duration Substrate (Thermo Scientific, Rockford, IL) according to the manufacturer's guidelines. Blots were imaged by ChemiDoc™ MP imaging system (Bio-rad) and densitometric analyses were performed using Image Lab software v4.1 (Bio-rad). The pixel densities in each band were normalized to the amount of β-actin (housekeeping) in that lane.

2.9. Quantitative real-time PCR (qRT-PCR)

qRT-PCR was carried out following our earlier protocols [19,20, 32–34]. Total RNAs were isolated from each retinal samples using Trizol reagent (Life Technologies, Grand Island, NY, USA) following manufacturer's instructions. RNase-free DNase I (Promega, USA) was used to remove any DNA contamination according to manufacturer's protocol. cDNAs were prepared from total RNA samples using reverse transcription by Oligo-dT primer along with Supercript III reverse tanscriptase (RT) (Life Technology, USA). In all of our experiments, no RT (without reverse transcriptase) was included as negative control for each sample. qRT-PCR of the samples were carried out using SYBR green and the CFX96 real-time cycler (Bio-Rad, Hercules, CA, USA). Each sample was measured in triplicate and normalized to housekeeping gene β-actin. Relative gene expression was analyzed using the ΔcT method (i.e. ΔcT = gene cT- β actin cT). Each treatment was determined using three to five eyes and data are shown as means ± SE. The primers used were: forward VEGF-A: 5′-AGCACAGCAGATGTGAATGC-3′, reverse VEGF-A: 5′-AATGCTTTCTCCGCTCTGAA-3′, forward VEGFR-2: 5′-TAAGGGCATGGAGTTCTTGG-3′, reverse VEGFR-2: 5′-CAGAGCAACACACCGAAAGA-3′, mouse actin forward: 5′-TGTTACCAACTGGGACGACA-3′; mouse actin reverse: 5′-CTTTTCACGGTTGGCCTTAG-3′.

2.10. Electron microscopic (EM) analysis

EMs on ultrathin plastic sections along the nasal/temporal plane was performed using an electron microscope (100CX; JEOL, Tokyo, Japan) as described previously [20,32]. The eyes were initially fixed in 2%/2% paraformaldehyde/glutaraldehyde at room temperature and followed by the careful removal of the cornea and lens from each eye. The eyecups were post fixed in 1% OsO_4 at room temperature. After staining, the eyes were rinsed with water and eyecups were embedded in Spurr's resin (Ted Pella Incorporated, Redding, CA, USA) for sectioning. Semi thin (0.75 μm) sections were stained with 1% toluidine blue in 1% sodium borate. One to three animals per group were analyzed. Ultrathin electron microscopy sections cut along the superior-inferior plane were post stained with uranyl acetate and lead citrate and imaged at ×25,000 using a JEOL 100CX electron microscope.

3. Results

3.1. miR200-b down-regulates VEGF in vitro

VEGF expression in DR is the key factor to regulate angiogenesis. miR200-b acts as an anti-angiogenic factor and is highly enriched in epithelial tissues. To elucidate the VEGF regulation by miR200-b, we first choose to test its effectiveness in an *in vitro* model (murine SVEC4-10), the primary cell target in DR. EC cells were transfected with pCAG-miR200-b-IRES-eGFP plasmid DNA complexed with lipofectamine 2000. Native eGFP fluorescence was assessed in transfected cells and compared with the untreated control (Fig. 1A). eGFP expression reflects the functional integrity of the plasmid DNA and the transfection ability of the lipofectamine mediated DNA complex.

In a parallel study, *VEGF* mRNA levels were evaluated in miR200-b transfected EC cells. We observed that the relative mRNA levels of endogenous VEGF-A (Fig. 1B) and VEGFR-2 (Fig. 1C) were significantly down-regulated in miR200-b transfected cells as measured by semi quantitative reverse transcriptase polymerase chain reaction (qRT-PCR) when compared to mock (lipofectamine only) treated controls. On the other hand, the untreated (endogenous) and mock control groups showed no alteration in *VEGF-A or VEGFR2* levels (Fig. 1B and C). All together these results define the anti-VEGF activity of miR200-b plasmid in EC cells.

3.2. miR200-b delayed wound repair

The wound-healing assay provides a valuable *in vitro* tool for validating the collective processes of cell migration, motility, and proliferation. To examine whether treatment of miR200-b exerts anti-angiogenic effects in wound healing in EC cells, we performed wound closure assays in SVEC EC cells. Untreated SVEC cells migrate faster toward the scratch than the miR200-b treated cells (Fig. 1D). Delivery of miR200-b significantly inhibited wound repair in SVEC cells within a day (24 h) after treatment with the pDNA (Fig. 1E). The angiogenesis can also be characterized by cell differentiation into capillaries and an *in vitro* tube formation or capillary formation (three dimensional structures) assay is well-established for predicting *in vivo* anti-angiogenesis. To analyze if miR200b could inhibit tubular network formation, SVEC cells were transfected with pCAG-miR200-b lipofectamine 2000 complexes. As shown in Fig. 2F, pCAG-miR200-b clearly inhibited

tube-like structures compared to the untreated control. Taken together, these results demonstrate that miR200-b has a negative effect on the angiogenic activity of EC cells.

3.3. miR200-b NPs prevent DR-associated vascular changes

Vascular abnormalities are sensitive indicators of DR. To examine whether intravitreal delivery of miR200-b DNA NPs could prevent retinal neovascularization and microaneurysms, we performed noninvasive fluorescence fundus imaging on *Ins2*^{Akita} mice at PI-3 m. Mock injected and age matched WT mice were used as controls. The results of the imaging clearly indicate that treatment with miR200-b DNA NPs can prevent vascular changes, including neovascularization and vascular leakage, compared with the mock injected controls (Fig. 2 and Fig. S2). We used ImageJ software to quantitatively measure the vasculature area on fundus images of *Ins2*^{Akita} mice. As shown in Fig. 3A and B, significant reduction in vasculature area is detected with pCAG-miR200-b NPs treated eyes when compared to age matched mock treated Akita. Consistent with the fluorescence angiography, recovery of the vascular area was comparable to values observed in age matchedWT. Thus NP-mediated reversal of retinal vascular damage could have a significant impact on the improvement of DR.

3.4. miR200-b NPs down-regulate retinal VEGF levels in aged Ins2^{Akita} mice

To investigate the anti-angiogenic activity of the pCAG-miR200-b DNA NPs to VEGF-directed angiogenesis, we measured VEGF A (Fig. 4A and B) and VEGFR-2 (Fig. 4A and C) expression in retinas isolated from P9m old *Ins2*^{Akita} mice. Western blots (Fig. 4A) demonstrated that VEGFR-2 expression was significantly down-regulated by the NPs compared to the mock injected controls (Fig. 4A and C). The VEGFR-2 level shows comparable values as aged matched WT controls (Fig. 4C). Results from these *in vivo* experiments were consistent with our *in vitro* results (Fig. 1C). However, interestingly, our *in vivo* experiments showed that the miR200-b NP formulation may more directly target VEGFR-2 than that of VEGF-A (Fig. 4), which plays a crucial role in endothelial development through cell proliferation and migration in angiogenesis. This observation is in agreement with the previous report [35].

3.5. miR200-b NPs treatments lead to ultrastructural improvements on retinal capillaries

Pathologically, retinal capillary wall breakdown, basement membrane thickening and death of capillary pericytes are early signs of DR. Fig. 5A presents a cartoon diagram of a capillary blood vessel cross section in WT mice. To determine the effects of miR200-b DNA NPs on the capillary structure and pathogenesis of DR in *Ins2*^{Akita} mice, we evaluated the ultrastructure of retinal capillaries in electron microscopic (EM) images taken from NP injected 9 month old *Ins2*^{Akita} mice (PI-3 m). Age matched uninjected WT and mock injected *Ins2*^{Akita} mice were used as controls (Fig. 5B and C). We show that the treatment with NPs improves pericyte coverage and decreases basement membrane thickness (Fig. 5D) compared to the mock treated *Ins2*^{Akita} (Fig. 5C and Fig. S3) control at PI-3 m.

4. Discussions

In the present study, we demonstrated for the first time the down-regulation of VEGFR-2 receptor after a single intravitreal administration of miR200-b DNA NPs under the control of the ubiquitous CAG promoter after 3 months post injection. We have shown that NP mediated therapeutic intervention can target the VEGFR-2 receptor and controls pathological clinical phenotype of angiogenesis.

VEGFs are a family of isoforms that are generated by alternative splicing of *VEGF* mRNA [10]. VEGF is produced by retinal vascular and neuroglia cells (e.g. Müller cells) and is a growth factor for the exudative and proliferative angiogenesis in DR. Among the four VEGF isoforms as found in humans, VEGF-A isoform binds to two cell surface autophosphorylating receptor tyrosine kinases (RTKs), VEGFR-1 (Flt-1) and VEGFR-2 (Flk-1/KDR) regulate the process of angiogenesis. VEGFR-2 is more potent than VEGFR-1 in stimulating endothelial cells [36]. VEGF binds and dimerizes two VEGFR-2 monomers that leads to receptor autophophorylation of VEGFR-2 tyrosine domains. These phosphotyrosines recruit several adaptor proteins that finally directs a wide spectrum of cellular signaling cascades like proliferation, migration and differentiations in EC cells [37]. The anti-apoptotic effect of VEGF in human umbilical vein EC cells was demonstrated *via* activation of VEGFR-2 but not with VEGFR-1 [10,38]. Studies have shown that the suppression of VEGFR-2, the primary signal transducer for angiogenesis, can block the VEGF-VEGFR-2 signaling pathway and leads to the inhibition of intraocular vascular leakage and neovascularization [39]. Other small molecule angiogenic inhibitors target VEGFR-2 to inhibit tumor growth, metastasis, and angiogenesis [40,41]. Therefore, VEGFR-2 is an important receptor for VEGF and an important target for anti-angiogenic therapy by inhibiting retinal neovascularization.

Currently, laser surgery and panretinal photocoagulation (PRP) therapies are available for the treatment of DR and age related macular degeneration. Multiple scattering laser treatments temporary shrink abnormal blood vessels. Recently, the FDA has approved several drugs for the treatment of DR like Eylea (Aflibercept, made of a human antibody fragment), and Lucentis (Ranibizumab, a monoclonal antibody fragment) that targets VEGF and works as anti-VEGF therapy. These drugs require monthly injections into the vitreous in order to maintain long-term effects. In addition, these drugs neutralize VEGF ligands in the blood stream and prevent the dimerization of VEGFR-2 receptors that consequently inhibit neovascularization. Therefore, there is clear demand for alternative and effective therapies to manage, control and reverse the ocular neovascularization phenotype seen in DR. To this end, our strategy is to target new retinal blood vessel formation by delivering miR200-b NPs into EC cells to knock down the expression of VEGFR-2. We showed that DNA NP-mediated miR200-b delivery can negatively regulate VEGFR-2 expression and inhibit intraocular pathological angiogenesis by inhibiting the VEGF-VEGFR-2 signaling pathway, with a safe and minimally invasive surgical procedure up to 3 months after a single intravitreal injection.

We have used EC cells for our initial investigation of miR200-b mediated down-regulation of VEGFR-2 in diabetes. We have chosen these cells, which are not a retinal cell line,

because they have been widely used as a model for studying EC abnormalities for other diseases such as neovascular proliferation in cancer [42]. The antiproliferative and vascular targeting consequences of the miR200-b plasmid DNA were validated *in vitro* in murine SVEC4-10 EC cells by a significant down regulation of cell proliferation, migration and tube formation. Studies have shown that the VEGFR-2 receptor directs the differentiation of EC cells into capillary tubes [39]. The potent activity of miR200-b in targeting VEGFR-2 to reduce retinal neovascularization was validated through a tube formation assay *in vitro* [15]. The EC migration, vacuolization and cell elongation in 3D gels was greatly inhibited by miR200-b treatment that directly reflects its VEGFR-2 targeting efficiency. VEGF ligand is needed to maintain the homeostasis of choriocapilaries, cones and ganglion cells in retina and consequently severe VEGF inhibition might result in structural disintegration and photoreceptor cell damage. Therefore, targeting and down regulation of VEGFR-2 is the key strategy of our current study by inhibiting neovascularization in a DR model.

Although chemical- and injury-induced models of retinal neovascularization exist, they are not able to mimic the chronic DR processes. The *Ins2*^{Akita} mouse is a common diabetic model to study VEGF dependent neovascularization resulting from hyperglycemia. *Ins2*^{Akita} possess a dominant point mutation in the gene encoding insulin-2 that leads to the misfolding of the insulin protein and established a monogenic model for studying non-insulin-dependent diabetes mellitus (DM). Previously, we [32] and others [43–45] have shown that the *Ins2*^{Akita} model presents increased retinal vascular permeability, apoptosis and produces early signs of DR. Our previous study indicated that *Ins2*^{Akita} mice develop hyperglycemia-associated vasculopathies and acts as a relevant model for later-onset DR with early and some late disease symptoms. We demonstrated that this mouse model exhibits early and late chronic DR signs and may be a suitable model for testing the therapeutics that are designed to target DR.

Naked plasmid DNA is unable to efficiently overcome numerous biological barriers in the cytoplasm. NPs can protect DNA from enzymatic cleavage. CK30PEG10k based DNA nanocompaction has been well-documented in retinal gene therapies by us and other groups as well. The CK30PEG10k mediated DNA NP formulations have been reported to be internalized into cells *via* nucleolin receptors [46,47]. Nucleolin is a cell surface receptor in angiogenic EC cells [48] and shuttles between the nucleus, cytoplasm and cell surface. Studies have shown that anti-angiogenic endostatin was taken up by the cells and transported into the nuclei of EC *via* nucleolin receptor and subsequently prevented growth and angiogenesis [49,50]. Therefore, the miR200-b DNA NP might be internalized and shuttled to the nucleus of EC cells *via* nucleolin receptors, subsequently expresses *miR200-b* that consequently knocks down VEGFR-2 expression as shown by both messenger and protein analyses (Fig. 4) and prevents neovascularization as indicated by fundus imaging (Figs. 2 and 3). Our *in vivo* results show that pCAG-miR200-b DNA NPs can prevent ocular neovascularization in the *Ins2-*^{Akita} model *via* suppression of VEGFR-2 activation. Human diabetic retinas have a reduction in the mir200-b level [15] that supports our miR200-b NP-mediated approach as a supplemental therapeutic for the treatment of DR to maintain vascular homeostasis in the diabetic retina. In this current study, we have demonstrated that miR200-b compacted DNA NPs injected *via* the intravitreal route might be a first line

therapeutic strategy for ocular neovascularization treatment and which may not need repetitive injections.

5. Conclusion

The development of nanotechnology has been growing in managing diabetes based on its success in other diseases like cancer [51]. Here we have shown that NP-mediated mir200-b delivery can protect the retina from retinal neovascularization by down regulating VEGFR-2 expression. This study provides important evidence of targeting VEGFR-2 by mir200-b in a hyperglycemic model of DR and might open up a potential therapeutic alternative in the management of VEGF-mediated neovascularization in DR.

Supplementary Material

Refer to Web version on PubMed Central for supplementary material.

Acknowledgments

This work was supported in part by of the U.S. National Institutes of Health, (R21EY024059-ZH and EY22778-MIN), the Harold Hamm Oklahoma Diabetes Center Talley award (Z.H.), the Oklahoma Center for the Advancement of Science and Technology (Z.H., M.I.N.), the Knights Templar Eye Foundation (Z.H.), the Carolina Center of Cancer Nanotechnology Excellence (Z.H.), the UNC Junior Faculty Development Award (Z.H.), and the Research to Prevent Blindness to the University of North Carolina Department of Ophthalmology (Z.H.). M.J.C. is an employee of Copernicus Therapeutics and holds stock in the company.

Appendix A. Supplementary data

Supplementary data to this article can be found online at http://dx.doi.org/10.1016/j.jconrel.2016.06.020.

References

1. Osaadon P, Fagan XJ, Lifshitz T, Levy J. A review of anti-VEGF agents for proliferative diabetic retinopathy. Eye (Lond). 2014; 28:510–520. [PubMed: 24525867]
2. Silva PS, Cavallerano JD, Sun JK, Aiello LM, Aiello LP. Effect of systemic medications on onset and progression of diabetic retinopathy. Nat Rev Endocrinol. 2010; 6:494–508. [PubMed: 20664533]
3. Rakoczy EP, Ali Rahman IS, Binz N, Li CR, Vagaja NN, de Pinho M, Lai CM. Characterization of a mouse model of hyperglycemia and retinal neovascularization. Am J Pathol. 2010; 177:2659–2670. [PubMed: 20829433]
4. Cai J, Boulton M. The pathogenesis of diabetic retinopathy: old concepts and new questions. Eye (Lond). 2002; 16:242–260. [PubMed: 12032713]
5. Curtis TM, Gardiner TA, Stitt AW. Microvascular lesions of diabetic retinopathy: clues towards understanding pathogenesis? Eye (Lond). 2009; 23:1496–1508. [PubMed: 19444297]
6. Lu M, Kuroki M, Amano S, Tolentino M, Keough K, Kim I, Bucala R, Adamis AP. Advanced glycation end products increase retinal vascular endothelial growth factor expression. J Clin Invest. 1998; 101:1219–1224. [PubMed: 9502762]
7. Adamis AP, Miller JW, Bernal MT, D'Amico DJ, Folkman J, Yeo TK, Yeo KT. Increased vascular endothelial growth factor levels in the vitreous of eyes with proliferative diabetic retinopathy. Am J Ophthalmol. 1994; 118:445–450. [PubMed: 7943121]

8. Aiello LP, Avery RL, Arrigg PG, Keyt BA, Jampel HD, Shah ST, Pasquale LR, Thieme H, Iwamoto MA, Park JE, et al. Vascular endothelial growth factor in ocular fluid of patients with diabetic retinopathy and other retinal disorders. N Engl J Med. 1994; 331:1480–1487. [PubMed: 7526212]
9. Hampton T. Scientists take aim at angiogenesis to treat degenerative eye diseases. JAMA. 2004; 291:1309–1310. [PubMed: 15026379]
10. Ferrara N, Gerber HP, LeCouter J. The biology of VEGF and its receptors. Nat Med. 2003; 9:669–676. [PubMed: 12778165]
11. Ferrara N, Carver-Moore K, Chen H, Dowd M, Lu L, O'Shea KS, Powell-Braxton L, Hillan KJ, Moore MW. Heterozygous embryonic lethality induced by targeted inactivation of the VEGF gene. Nature. 1996; 380:439–442. [PubMed: 8602242]
12. Fong GH, Rossant J, Gertsenstein M, Breitman ML. Role of the Flt-1 receptor tyrosine kinase in regulating the assembly of vascular endothelium. Nature. 1995; 376:66–70. [PubMed: 7596436]
13. Deiuliis JA. MicroRNAs as regulators of metabolic disease: pathophysiologic significance and emerging role as biomarkers and therapeutics. Int J Obes. 2015
14. Friedman RC, Farh KK, Burge CB, Bartel DP. Most mammalian mRNAs are conserved targets of microRNAs. Genome Res. 2009; 19:92–105. [PubMed: 18955434]
15. McArthur K, Feng B, Wu Y, Chen S, Chakrabarti S. MicroRNA-200b regulates vascular endothelial growth factor-mediated alterations in diabetic retinopathy. Diabetes. 2011; 60:1314–1323. [PubMed: 21357793]
16. Choi YC, Yoon S, Jeong Y, Yoon J, Baek K. Regulation of vascular endothelial growth factor signaling by miR-200b. Mol Cell. 2011; 32:77–82.
17. Yin H, Kanasty RL, Eltoukhy AA, Vegas AJ, Dorkin JR, Anderson DG. Non-viral vectors for gene-based therapy. Nat Rev Genet. 2014; 15:541–555. [PubMed: 25022906]
18. Han Z, Conley SM, Naash MI. AAV and compacted DNA nanoparticles for the treatment of retinal disorders: challenges and future prospects. Invest Ophthalmol Vis Sci. 2011; 52:3051–3059. [PubMed: 21558483]
19. Han Z, Banworth MJ, Makkia R, Conley SM, Al-Ubaidi MR, Cooper MJ, Naash MI. Genomic DNA nanoparticles rescue rhodopsin-associated retinitis pigmentosa phenotype. FASEB J Off Publ Fed Amer Socie Exper Biol. 2015
20. Han Z, Conley SM, Makkia RS, Cooper MJ, Naash MI. DNA nanoparticle-mediated ABCA4 delivery rescues Stargardt dystrophy in mice. J Clin Invest. 2012; 122:3221–3226. [PubMed: 22886305]
21. Han Z, Koirala A, Makkia R, Cooper MJ, Naash MI. Direct gene transfer with compacted DNA nanoparticles in retinal pigment epithelial cells: expression, repeat delivery and lack of toxicity. Nanomedicine (London). 2012; 7:521–539.
22. Koirala A, Conley SM, Naash MI. Episomal maintenance of S/MAR-containing non-viral vectors for RPE-based diseases. Adv Exp Med Biol. 2014; 801:703–709. [PubMed: 24664761]
23. Koirala A, Makkia RS, Conley SM, Cooper MJ, Naash MI. S/MAR-containing DNA nanoparticles promote persistent RPE gene expression and improvement in RPE65-associated LCA. Hum Mol Genet. 2013
24. Koirala A, Makkia RS, Cooper MJ, Naash MI. Nanoparticle-mediated gene transfer specific to retinal pigment epithelial cells. Biomaterials. 2011; 32:9483–9493. [PubMed: 21885113]
25. Cai X, Conley SM, Nash Z, Fliesler SJ, Cooper MJ, Naash MI. Gene delivery to mitotic and postmitotic photoreceptors via compacted DNA nanoparticles results in improved phenotype in a mouse model of retinitis pigmentosa. FASEB J Off Publ Feder Amer Socie Exp Biol. 2010; 24:1178–1191.
26. Cai X, Nash Z, Conley SM, Fliesler SJ, Cooper MJ, Naash MI. A partial structural and functional rescue of a retinitis pigmentosa model with compacted DNA nanoparticles. PLoS One. 2009; 4:e5290. [PubMed: 19390689]
27. Ziady AG, Gedeon CR, Miller T, Quan W, Payne JM, Hyatt SL, Fink TL, Muhammad O, Oette S, Kowalczyk T, Pasumarthy MK, Moen RC, Cooper MJ, Davis PB. Transfection of airway epithelium by stable PEGylated poly-L-lysine DNA nanoparticles in vivo. Mol Ther. 2003; 8:936–947. [PubMed: 14664796]

28. Fink TL, Klepcyk PJ, Oette SM, Gedeon CR, Hyatt SL, Kowalczyk TH, Moen RC, Cooper MJ. Plasmid size up to 20 kbp does not limit effective in vivo lung gene transfer using compacted DNA nanoparticles. Gene Ther. 2006; 13:1048–1051. [PubMed: 16525478]
29. Ding XQ, Quiambao AB, Fitzgerald JB, Cooper MJ, Conley SM, Naash MI. Ocular delivery of compacted DNA-nanoparticles does not elicit toxicity in the mouse retina. PLoS One. 2009; 4:e7410. [PubMed: 19823583]
30. Liu G, Li D, Pasumarthy MK, Kowalczyk TH, Gedeon CR, Hyatt SL, Payne JM, Miller TJ, Brunovskis P, Fink TL, Muhammad O, Moen RC, Hanson RW, Cooper MJ. Nanoparticles of compacted DNA transfect postmitotic cells. J Biol Chem. 2003; 278:32578–32586. [PubMed: 12807905]
31. Farjo R, Skaggs J, Quiambao AB, Cooper MJ, Naash MI. Efficient non-viral ocular gene transfer with compacted DNA nanoparticles. PLoS One. 2006; 1:e38. [PubMed: 17183666]
32. Han Z, Guo J, Conley SM, Naash MI. Retinal angiogenesis in the Ins2(Akita) mouse model of diabetic retinopathy. Invest Ophthalmol Vis Sci. 2013; 54:574–584. [PubMed: 23221078]
33. Mitra RN, Han Z, Merwin M, Al Taai M, Conley SM, Naash MI. Synthesis and characterization of glycol chitosan DNA nanoparticles for retinal gene delivery. ChemMedChem. 2014; 9:189–196. [PubMed: 24203490]
34. Zheng M, Mitra RN, Filonov NA, Han Z. Nanoparticle-Mediated Rhodopsin cDNA but not Intron-Containing DNA Delivery Causes Transgene Silencing in a Rhodopsin Knockout Model. FASEB J. 2015
35. Chan YC, Roy S, Khanna S, Sen CK. Downregulation of endothelial microRNA-200b supports cutaneous wound angiogenesis by desilencing GATA binding protein 2 and vascular endothelial growth factor receptor 2. Arterioscler Thromb Vasc Biol. 2012; 32:1372–1382. [PubMed: 22499991]
36. Yoshihara T, Takahashi-Yanaga F, Shiraishi F, Morimoto S, Watanabe Y, Hirata M, Hoka S, Sasaguri T. Anti-angiogenic effects of differentiation-inducing factor-1 involving VEGFR-2 expression inhibition independent of the Wnt/beta-catenin signaling pathway. Mol Cancer. 2010; 9:245. [PubMed: 20843378]
37. Shibuya M. Vascular endothelial growth factor (VEGF) and its receptor (VEGFR) signaling in angiogenesis: a crucial target for anti- and pro-angiogenic therapies. Genes Cancer. 2011; 2:1097–1105. [PubMed: 22866201]
38. Gerber HP, McMurtrey A, Kowalski J, Yan M, Keyt BA, Dixit V, Ferrara N. Vascular endothelial growth factor regulates endothelial cell survival through the phosphatidylinositol 3′-kinase/Akt signal transduction pathway. Requirement for Flk-1/KDR activation. J Biol Chem. 1998; 273:30336–30343. [PubMed: 9804796]
39. Kim JH, Kim MH, Jo DH, Yu YS, Lee TG, Kim JH. The inhibition of retinal neovascularization by gold nanoparticles via suppression of VEGFR-2 activation. Biomaterials. 2011; 32:1865–1871. [PubMed: 21145587]
40. Yakes FM, Chen J, Tan J, Yamaguchi K, Shi Y, Yu P, Qian F, Chu F, Bentzien F, Cancilla B, Orf J, You A, Laird AD, Engst S, Lee L, Lesch J, Chou YC, Joly AH. Cabozantinib (XL184), a novel MET and VEGFR2 inhibitor, simultaneously suppresses metastasis, angiogenesis, and tumor growth. Mol Cancer Ther. 2011; 10:2298–2308. [PubMed: 21926191]
41. Niu G, Chen X. Vascular endothelial growth factor as an anti-angiogenic target for cancer therapy. Curr Drug Targets. 2010; 11:1000–1017. [PubMed: 20426765]
42. Jain N, Miu B, Jiang JK, McKinstry KK, Prince A, Swain SL, Greiner DL, Thomas CJ, Sanderson MJ, Berg LJ, Kang J. CD28 and ITK signals regulate autoreactive T cell trafficking. Nat Med. 2013; 19:1632–1637. [PubMed: 24270545]
43. Barber AJ, Antonetti DA, Kern TS, Reiter CE, Soans RS, Krady JK, Levison SW, Gardner TW, Bronson SK. The $Ins2^{Akita}$ mouse as a model of early retinal complications in diabetes. Invest Ophthalmol Vis Sci. 2005; 46:2210–2218. [PubMed: 15914643]
44. McLenachan S, Magno AL, Ramos D, Catita J, McMenamin PG, Chen FK, Rakoczy EP, Ruberte J. Angiography reveals novel features of the retinal vasculature in healthy and diabetic mice. Exp Eye Res. 2015; 138:6–21. [PubMed: 26122048]

45. Wright WS, Yadav AS, McElhatten RM, Harris NR. Retinal blood flow abnormalities following six months of hyperglycemia in the Ins2(Akita) mouse. Exp Eye Res. 2012; 98:9–15. [PubMed: 22440813]

46. Chen X, Kube DM, Cooper MJ, Davis PB. Cell surface nucleolin serves as receptor for DNA nanoparticles composed of pegylated polylysine and DNA. Mol Ther. 2008; 16:333–342. [PubMed: 18059369]

47. Chen X, Shank S, Davis PB, Ziady AG. Nucleolin-mediated cellular trafficking of DNA nanoparticle is lipid raft and microtubule dependent and can be modulated by glucocorticoid. Molecular therapy: the journal of the American Society of Gene Therapy. 2011; 19:93–102. [PubMed: 20959809]

48. Christian S, Pilch J, Akerman ME, Porkka K, Laakkonen P, Ruoslahti E. Nucleolin expressed at the cell surface is a marker of endothelial cells in angiogenic blood vessels. J Cell Biol. 2003; 163:871–878. [PubMed: 14638862]

49. Fu Y, Chen Y, Luo X, Liang Y, Shi H, Gao L, Zhan S, Zhou D, Luo Y. The heparin binding motif of endostatin mediates its interaction with receptor nucleolin. Biochemistry. 2009; 48:11655–11663. [PubMed: 19877579]

50. Shi H, Huang Y, Zhou H, Song X, Yuan S, Fu Y, Luo Y. Nucleolin is a receptor that mediates antiangiogenic and antitumor activity of endostatin. Blood. 2007; 110:2899–2906. [PubMed: 17615292]

51. Li Z, Rana TM. Therapeutic targeting of microRNAs: current status and future challenges. Nat Rev Drug Discov. 2014; 13:622–638. [PubMed: 25011539]

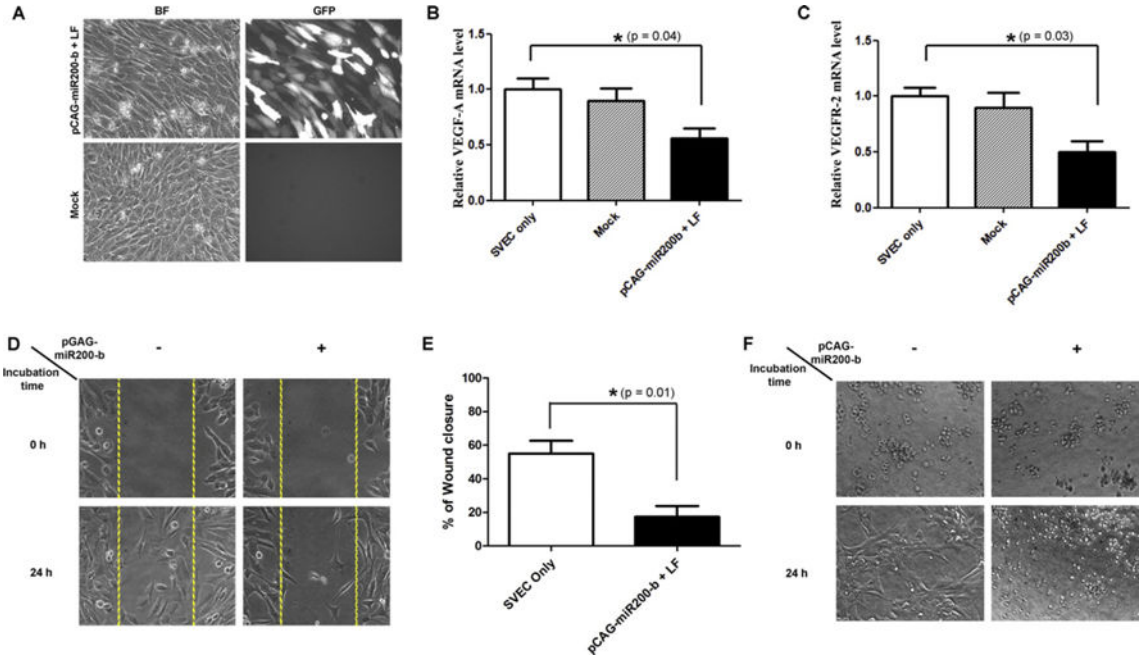

Fig. 1.

(A) *In vitro* transfection of pCAG-miR200-b-IRES-eGFP with lipofectamine 2000 (mock, top panel) and without lipofectamine (bottom panel) in SVEC cells. Left and right rows represent images taken in bright field (BF) and GFP channel, respectively. (B) Relative VEGF-A mRNA expression (n = 3). (C) Relative VEGFR-2 mRNA expression (n = 3). Quantitative analyses were analyzed by measuring mRNA expression relative to housekeeping beta actin. Significance was measured with one-way ANOVA analysis with Bonferroni multiple comparison test (B & C). Each value represents the mean (±SEM). (D) SVEC cells transfected with pCAG-miR200-b-IRSE-eGFP pDNA exhibited significant migration compared to the untreated control after creating the wounds (market by yellow margin). (E) Differences in the migrations of EC cells (i.e. wound healing) were statistically significant. The extent of wound closure was determined by measuring the wound area healed with miR200-b treatments compared with the initial wound area (n = 3, *P < 0.05). Untreated cells were taken as control under the same experimental condition. Significance was measured with *t*-test and each value represents the mean ± SEM. (F) The representative morphogenic responses of SVEC cells cultured onto 3D-matrigel after transfection with pDNA (right panel) and without treatment (left panel). Images were taken after 0 and 24 h of seeding onto matrigel. Images (A, D & F) were captured at 20× using Axioscope; Carl Zeiss Meditec, Jena, Germany.

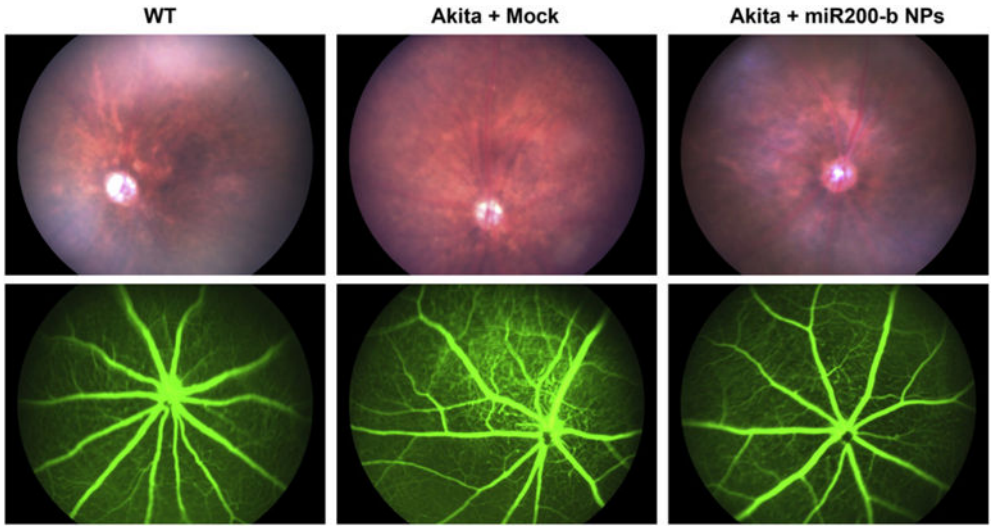

Fig. 2.

Fluorescein angiography shows the inhibition of retinal neovascularization in male *Ins2*^{Akita} animals treated at 9 months of age and assessed at 3 months post injection (PI-3 m) with miR200-b DNA NPs and compared with the age matched mock (pCAG-IRES-eGFP) injected positive control. Age matched and untreated wild type (WT) mice were taken as negative control. Top and bottom panels represent photographs from bright field and GFP channel.

Fig. 3.

(A–B) Vascular area was determined by considering the area occupied by the green fluorescence and quantified by NIH Image J software for each separate eye. Values are presented as mean ± SEM and are significantly different (*P < 0.05). Significance was measured by one-way ANOVA (n = 3). The mock, in this study, represents the injection of the pCAG-IRES-eGFP in endotoxin free saline.

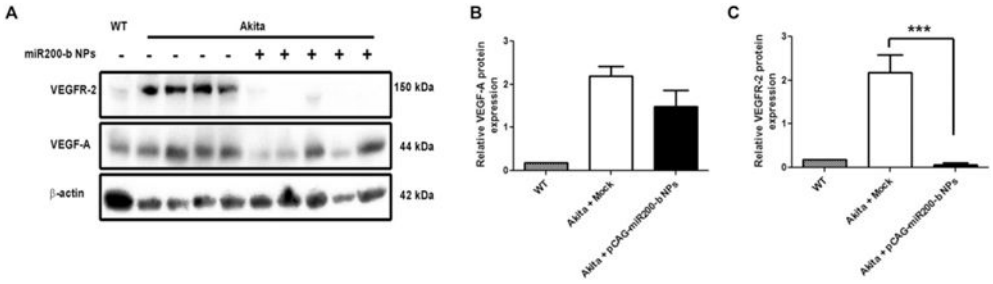

Fig. 4.

(A) Western blot analysis of VEGFR-2 and VEGF-A proteins. miR200-b DNA NP injected eyes showed significant amounts of VEGFR-2 down-regulation. (B–C) Relative expression of VEGF-A and VEGFR-2 proteins from untreated WT, mock (pCAG-IRES-eGFP) treated *Ins2*^{Akita} and NP injected *Ins2*^{Akita} mice at 3 months post injections. All mice were age matched and injected at 6 months of age. Values are presented as mean ± SE and are significantly different (***P < 0.001). Significance was measured by one-way ANOVA (n = 4).

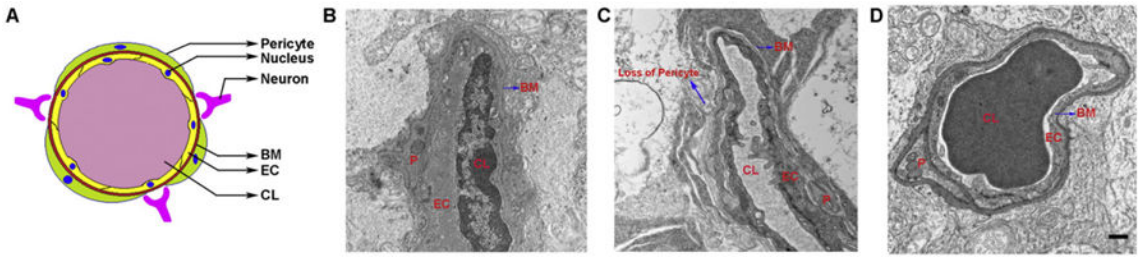

Fig. 5.

(A) A cartoon diagram of a transverse section of retinal capillary structure. Representative transmission electron micrographs (EM) of retinal capillaries from the outer plexiform layer of age matched (B) WT (untreated), and (C) *Ins2*$^{\text{Akita}}$ (pCAG-IRES-eGFP mock injected). There is a loss of pericytes found in the mock treated *Ins2*^{Akita} capillary structure, and (D) DNA NP-miR200-b injected retinas. BM: basement membrane, EC: endothelial cell, CL: capillary lumen, P: pericyte (Note: pericytes share their basement membrane with retinal EC cells). Scale bar = 500 nm.